ISSN 1674-1056
http://cpb.iphy.ac.cn
http://iopscience.iop.org/cpb
中国物理 B
Chinese Physics
中国物理
Chinese Physics B

Electro-statically controllable graphene local heater

Hui-Shan Wang(王慧山), Lian-Wen Deng(邓联文), Lei Li(李蕾), Qiu-Juan Sun(孙秋娟), Hong Xie(谢红), Hao-Min Wang(王浩敏)
Citation: Chin. Phys. B . 2018, 27(3): 037203. **doi:** 10.1088/1674-1056/27/3/037203

Journal homepage: http://cpb.iphy.ac.cn; http://iopscience.iop.org/cpb

What follows is a list of articles you may be interested in

A self-powered sensitive ultraviolet photodetector based on epitaxial graphene on silicon carbide

Jiao Huang(黄郊), Li-Wei Guo(郭丽伟), Wei Lu(芦伟), Yong-Hui Zhang(张永晖), Zhe Shi(史哲), Yu-Ping Jia(贾玉萍), Zhi-Lin Li(李治林), Jun-Wei Yang(杨军伟), Hong-Xiang Chen(陈洪祥), Zeng-Xia Mei(梅增霞), Xiao-Long Chen(陈小龙)
Chin. Phys. B . 2016, 25(6): 067205. **doi:** 10.1088/1674-1056/25/6/067205

Transport properties of zigzag graphene nanoribbons adsorbed with single iron atom

Yang Yu-E, Xiao Yang, Yan Xiao-Hong, Dai Chang-Jie
Chin. Phys. B . 2015, 24(11): 0117204. **doi:** 10.1088/1674-1056/24/11/117204

Tunneling magnetoresistance based on a Cr/graphene/Cr magnetotunnel junction

Luan Gui-Ping, Zhang Pei-Ran, Jiao Na, Sun Li-Zhong
Chin. Phys. B . 2015, 24(11): 0117201. **doi:** 10.1088/1674-1056/24/11/117201

Spin transport in a Zigzag normal/ferromagnetic graphene junction

Shi Hao-Sheng, Vahram L. Grigoryan
Chin. Phys. B . 2015, 24(5): 057202. **doi:** 10.1088/1674-1056/24/5/057202

Synthesis and electrochemical properties of three-dimensional graphene/polyaniline composites for supercapacitor electrode materials

Zhao Wen, He Da-Wei, Wang Yong-Sheng, Du Xiang, Xin Hao
Chin. Phys. B . 2015, 24(4): 047204. **doi:** 10.1088/1674-1056/24/4/047204

Electro-statically controllable graphene local heater*

Hui-Shan Wang(王慧山)[1,3,4], Lian-Wen Deng(邓联文)[2,†], Lei Li(李蕾)[2], Qiu-Juan Sun(孙秋娟)[2], Hong Xie(谢红)[1,3], and Hao-Min Wang(王浩敏)[1,3,‡]

[1] State Key Laboratory of Functional Materials for Informatics, Shanghai Institute of Microsystem and Information Technology, Chinese Academy of Sciences, Shanghai 200050, China

[2] School of Physics and Electronics, Central South University, Changsha 410083, China

[3] CAS Center for Excellence in Superconducting Electronics, Chinese Academy of Sciences, Shanghai 200050, China

[4] School of Electronic, Electrical and Communication Engineering, University of Chinese Academy of Sciences, Beijing 100049, China

(Received 12 October 2017; revised manuscript received 18 December 2017; published online 11 February 2018)

We report on current-induced thermal power investigation of graphene nanostructure for potential local-heating applications. It is found that the efficiency of heating can be greatly improved if graphene is patterned into structures with narrow width and long channel. In a narrow graphene-ribbon, the Joule heating power exhibits an obvious dependence on the back-gate voltage. By monitoring Raman spectra, the temperature of graphene-ribbon can be determined. The temperature of graphene-ribbon is modulated by the electric field effect when the sample is sourced with a relatively high current.

Keywords: graphene, electric field effect, Raman

PACS: 72.80.Vp, 73.20.At, 74.25.nd **DOI:** 10.1088/1674-1056/27/3/037203

1. Introduction

The discovery of graphene[1] has inspired intense research activities in the novel two-dimensional (2D) carbon based electronic system. Electronic transport in graphene is greatly different from that in the conventional 2D electronic systems owing to the linear energy dispersion relationship at the Dirac point in its electronic band structure.[2,3] When graphene is patterned into narrow ribbons, electronic quantum confinement may make the narrow ribbons into semiconductors species. Normally, only when the width of the nano-ribbon is scaled down to at least 5 nm, the opening of an energy gap bigger than 0.3 eV is expected.[4] Lithographic patterning of graphene sheets can obtain graphene ribbons with widths down to $\sim$ 20 nm so far[5,6] and edge roughness of $\sim$ 5 nm, and the width is very difficult to narrow further via existing cutting-edge top-down approaches. As such, the application of graphene as semiconductor may need much more efforts and more time than what people expected. Recently, it is found that graphene[7] and graphene nano-ribbon[8] exhibit a remarkable current carrying capacity on the order of 10^8 A/cm^2. This superior current-carrying capacity is regarded as the key characteristics for possible application in on-chip electrical interconnects. Actually, both graphene and its ribbon have a relatively high resistivity, which is electro-statically controllable. As such, the high current-carrier-capacity could give graphene and its ribbon more opportunities in the thermal application.

Graphene heaters in large-scale can be used in automobile windows, mirrors, memory devices, and displays.[9–11] More recently, the heaters based on graphene materials were fabricated on flexible[12,13] and insulating substrates.[14] In addition, investigation about phonon scattering or black body radiation was carried out in graphene.[15–17] As such, further investigations on the graphene based nano-heater will definitely offer an innovative and wide-ranging platform for creative basic and applied research in thermal nanotechnology. In this work, it is experimentally shown that graphene nanostructures can be an electrostatically controllable local heater.

2. Methods

The graphene films are synthesized on Cu foil by chemical vapor deposition (CVD).[18] Figure 1(a) shows an atomic force microscope (AFM) image of an edge of graphene transferred onto the silicon substrate with 300 nm of thermal SiO_2. The line-scan of profile shows that the graphene film has a height of about 0.532 nm, which is consistent with the thickness of a monolayer.[19] Raman spectrum is taken by a 633 nm He–Ne laser with the power less than 1 mW to evaluate the quality of the CVD graphene, and the spot size of the laser is about 1 μm. As shown in Fig. 1(b), the Raman spectrum includes two strong peaks, namely, G and 2D, located at the

*Project supported by the National Key R&D Program of China (Grant No. 2017YFF0206106), the Chinese Academy of Sciences (Grant No. XDB04040300), the National Natural Science Foundation of China (Grant No. 51772317), and the Science and Technology Commission of Shanghai Municipality, China (Grant No. 16ZR1442700).

†Corresponding author. E-mail: denglw@csu.edu.cn

‡Corresponding author. E-mail: hmwang@mail.sim.ac.cn

© 2018 Chinese Physical Society and IOP Publishing Ltd

wavenumbers of 1587.7 cm^{-1} and 2688.7 cm^{-1}, respectively. And an ignorable peak near 1345.3 cm^{-1} (known as D peak) proves that the quality of the graphene is not obviously degraded after transfer. The process flow of device fabrication is outlined in Fig. 1(c). Once the CVD graphene film has been transferred, the next step is to electrically contact graphene with metal electrodes using standard e-beam lithography. Electrodes of 10/50-nm-Ti/Au are fabricated on top of the graphene samples, and then, graphene is patterned by a standard lithography and following oxygen plasma etching. All the devices are annealed at 300 °C in Ar/H_2 for 6 hours to remove adsorbates and contaminants introduced in the fabrication procedure. The finished devices are then ready to be wire-bonded and measured.

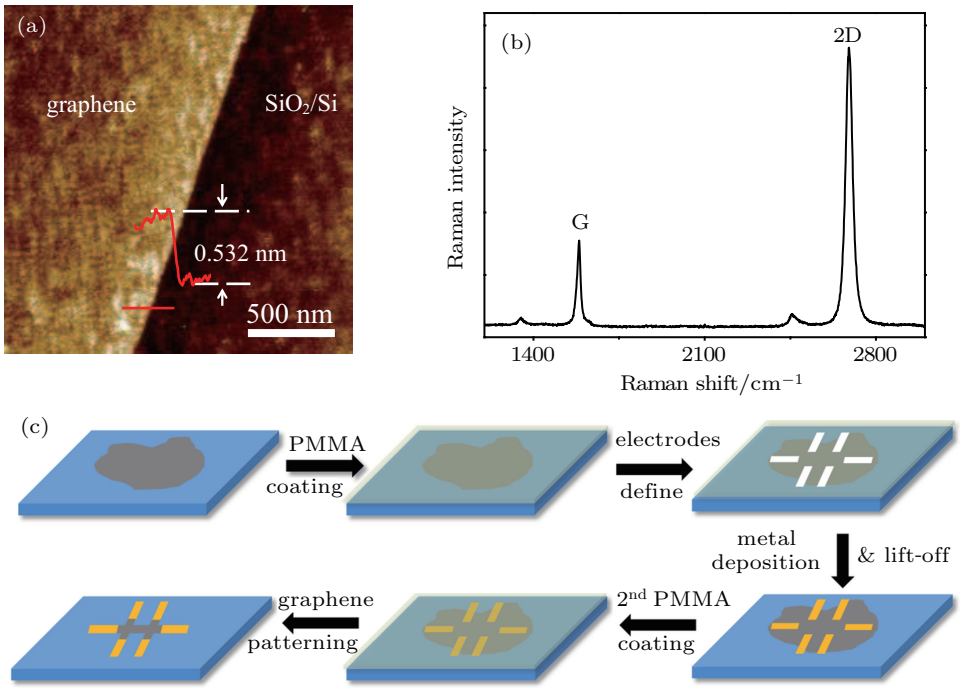


Fig. 1. (color online) (a) Atomic force image showing an edge of CVD graphene sheet transferred on SiO_2/Si substrate. (b) Raman spectrum of the monolayer CVD graphene. (c) Schematic diagram gives the process steps to make graphene based devices.

3. Results and discussion

Graphene could carry very high electrical currents without sustaining damage.[20] So applying a source-drain of a few volts across the samples is a very effective way to examine the quality of CVD graphene. Figure 2(a) shows the schematic of the two-terminal graphene field effect transistor (GFET), and all the graphene channels have a width of 5 μm and a length of 10 μm. To avoid the oxidization and preserve the integrity of the device in the high bias regime, measurements of *I*–*V* characteristics are carried out in vacuum (10^{-5} mbar). During the measurement, the back-gate voltage is kept at zero. The *I*–*V* curves of six graphene samples are recorded to investigate electrical breakdown, and then plotted in Fig. 2(b). It is found that the *I*–*V* curve is increasing linearly at low bias from 0 to 0.5 V, as shown in Fig. 2(c) and then exhibits a trend to saturate at higher bias, which is caused by the self-heating effects.[21] It is found that all the devices break down at about 5–6 mA. We plot the breakdown current density in Fig. 2(d). It is found that the breakdown current density J is between 3.0 A/cm^2 and 3.5×10^8 A/cm^2 for all samples. The value is quite near to the breakdown current density of the exfoliated graphene. It indicates that the CVD graphene here has a very high current-carrying capacity similar to the exfoliated graphene. The SEM images of the devices after breakdown are shown in Fig. S1 of supplementary information. The results indicate that breakdown mainly happens in the graphene channel.

To understand the influence of the device configuration on the dissipated electrical power, we compare the scaled current density $J = I/(Wd)$ in two devices, a wide device with wide $W = 1$ μm and a ribbon device with $W = 100$ nm. Here, I represents the current sourced, and d represents the thickness of the graphene, which is chosen to be 0.34 nm. The wide one has a channel length of 3 μm, as shown in the inset of Fig. 3(a), and the ribbon heater has a zigzag channel with a length of 10 μm, as shown in the inset of Fig. 3(b). The nano-ribbon device can be obtained by patterning the wide one. Figure 3 shows the gate dependence of Joule heating characteristics for the two graphene-heater devices. We employ a four-point configuration to avoid the contribution of the contact resistance at

the graphene-electrode interfaces.[22,23] As shown in Fig. 3, Joule heating power has an obvious dependence on the back-gate voltage in both devices. Although the Joule heating power geometrically increases with the rising of the current density, the modulability of the gate bias decreases in both devices. In addition, an increase of device length L and a decrease of device width W bring an increased resistance and therefore a decreased current. As shown in Fig. 3(a), the maximum power of the wide device locates near 20 V while that of the ribbon is near 0 V (see Fig. 3(b)). The devices are a little bit p-type doped from the substrates and absorbates.[24] For the ribbon devices, the geometry is not well approximated by a parallel plate capacitor any more. The local electrical field around the nano-ribbon is very strong. The gate has more efficient modulation on the nano-ribbon. From these data, we find that the ~ 100 nm wide graphene nano-ribbon shows higher power than a wide device when operated at a similar current density. The reason is that the introduction of edges increases the charge-carriers' scattering in graphene, and therefore increases the sheet resistance (see Fig. S2 in supplementary information). If we wish to increase the efficiency of Joule heating further, we can increase the device length or narrow-down the graphene ribbon, with the trade-off of an increased sheet resistance and therefore an increased heating power. Beside, treatment by plasma or ion beam[25] is another efficient way to increase the sheet resistance. At the same time, the zigzag pattern can also bring graphene more tolerance for its mechanical deformation.

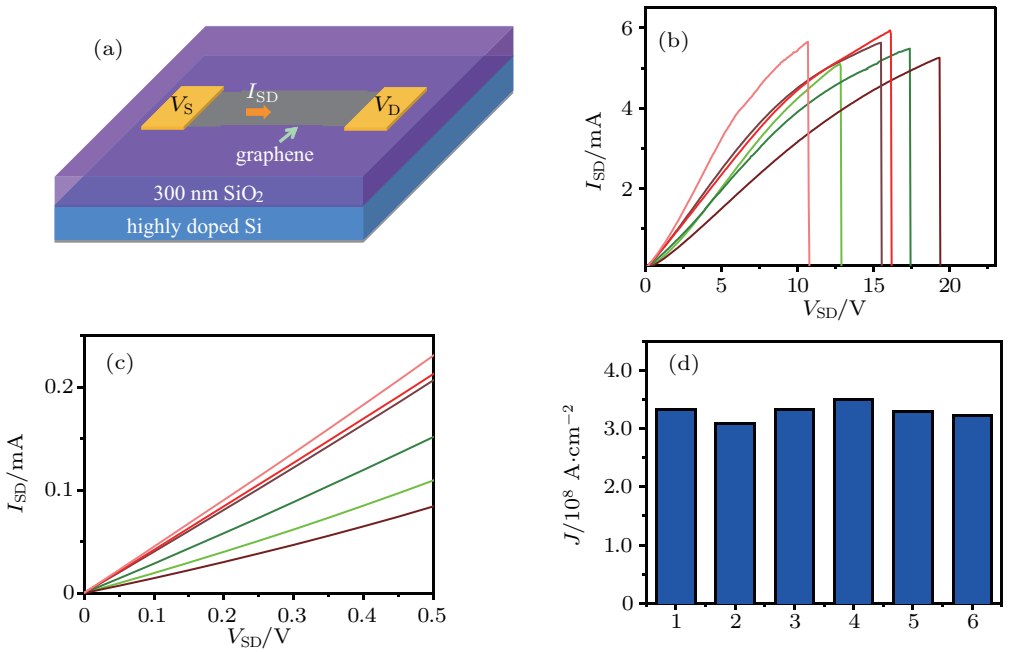


Fig. 2. (color online) (a) Schematic of two-terminal graphene field effect transistor (GFET). (b) I–V curves of six graphene samples taken through electrical breakdown. All graphene channels have a width of 5 μm and a length of 10 μm. (c) I–V measurement from 0 to 0.5 V. (d) The breakdown current density J of the six samples.

Subsequently, a Raman spectroscopy-based technique is used to determine the temperature of the graphene samples. Graphene normally exhibits clear signatures in Raman spectra[26,27] and its Raman peaks also manifest a strong temperature dependence.[28–30] The high temperature sensitivity of the peaks allows one to monitor the local temperature change produced by Joule heating on the graphene sample. In advance, we calibrate the temperature dependence of the Raman 2D peak for the graphene ribbon shown in Fig. 3(b). The Raman measurements are also performed in a back-scattering configuration with the 633-nm line laser as exciting radiation. We also examine the temperature dependence of the G and D bands of the graphene sample (see Fig. S3 in supplementary information). Among the D, G, and 2D peaks of graphitic materials, the 2D peak usually has the most obvious shift.[30] As such, we adopt the 2D peak for the investigation. The graphene temperature can be controlled using a hot plate. When the temperature of the examined sample varies in the range from 300 K to 550 K with 50 K intervals, its Raman spectra are recorded as shown in Fig. 4(a). Figure 4(a) presents the 2D peak shapes and positions for the ribbon at different temperatures. All the data are recorded only after 5 min when the 2D peak shifts no more, which indicates that the device has reached its thermal equilibrium. The 2D peak shifts toward the lower frequency with the increase of the temperature. The 2D peak positions are extracted and plotted in

Fig. 4(b). As shown in Fig. 4(b), the relationship of the 2D-peak position and temperature can be described by a linear formula $\omega_{2D} \approx 2709.5 - 0.062T$. Similar to the G band,[29] the influence of the temperature on 2D phonon modes includes two components, the intrinsic temperature contribution due to the anharmonicities of the phonon modes and the volume contribution caused by the thermal expansion of the crystal. The former dominates the 2D phonon mode in normal condition. The extracted temperature coefficient is about 0.062±0.005. The full Raman spectra of Fig. 4(a) are shown in Fig. S3 of supplementary information. The observed linear trend of the 2D-peak is consistent with that for other carbon-based materials.[30–34] Table S1 summarizes the temperature coefficient of 2D peak for carbon-based materials.

In the next-step experiment, the ribbon sample is sourced with a current with a density of 4.5×10^7 A/cm^2. Simultaneously, the Raman spectra of 2D band are recorded for the graphene heater when the Joule heating power is modulated by the electric field effect. As shown in Fig. 4(c), the 2D peak position is remarkably modulated by the gate voltage (see details in Fig. S4). The 2D peak position locates at 2690 cm^{-1}, 2683 cm^{-1}, 2669 cm^{-1}, 2679 cm^{-1}, and 2692 cm^{-1}, respectively, when the back gate is set to −20 V, −10 V, 0 V, 10 V, and 20 V. The temperature of the graphene heater is estimated from the above relationship of power dissipation vs. temperature. The corresponding temperature is about 305 K, 418 K, 640 K, 478 K, and 315 K, respectively. It should be noted that although the 2D band of graphene could be influenced by the electric field effect (EFE), the EFE leads to a minor shift of the 2D peak position (less than 5 cm^{-1}) when the gate voltage (V_g) sweeps from neutral point to high gate bias (±80 V).[35] Furthermore, the shift caused by EFE is in opposite direction. Here, it is believed that the SiO_2 substrate below the graphene channel is responsible for most of the heat dissipation, and the other is carried to the graphene that extends beyond the device and metallic contacts. The efficient thermal coupling between graphene and silicon oxide also exists via hot-electron remote-scattering of polar surface phonons.[15] In this experiment, the 2D peak of graphene shifts by about 20 cm^{-1}. At room temperature, we do not find the Raman peak shift caused by gating (see Fig. S5 in supplementary information). As such, the dominant contribution of the 2D-peak shift comes from the change of temperature. As the experiments are carried out in ambient temperature, only the device temperature above room temperature can be recorded.

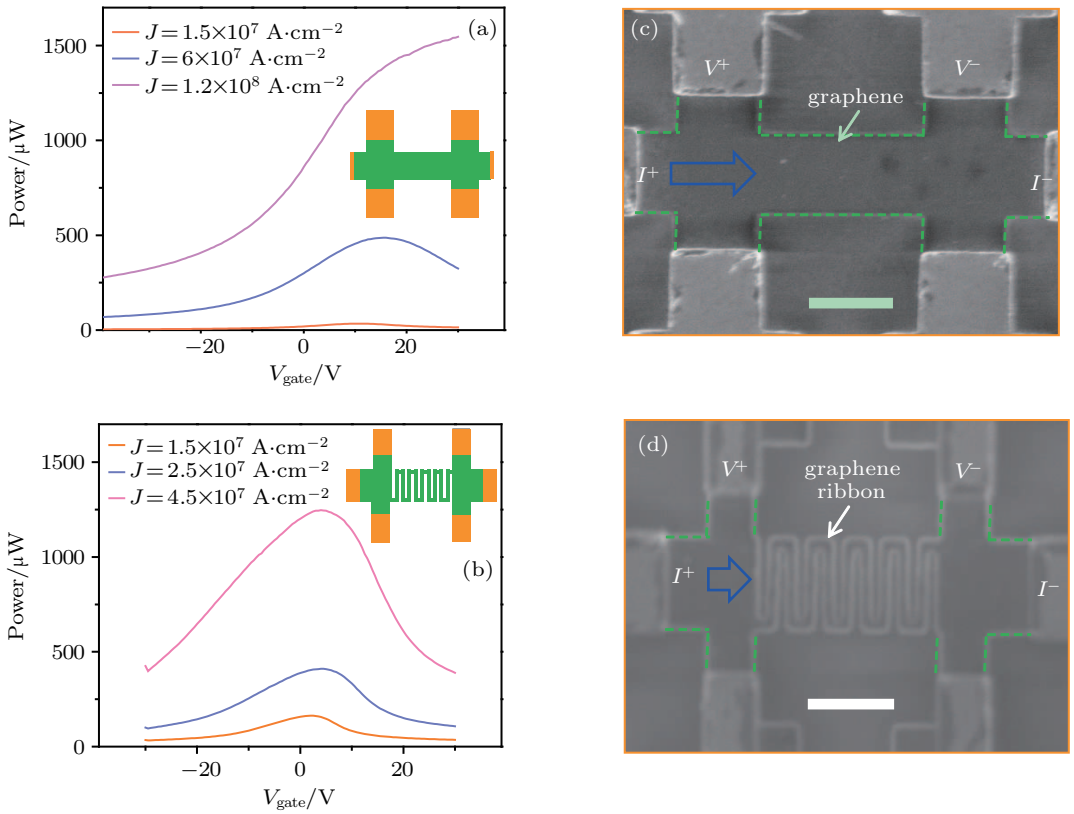


Fig. 3. (color online) The gate dependence of Joule heating power under different current densities in the graphene heater (a) with a channel width of 1 μm or (b) with a zigzag channel (the channel has a width of 100 nm and a length of 10 μm). The inset shows schematics of the corresponding devices. Panels (c) and (d) show the SEM images of the real devices. The scale bar is 1 μm.

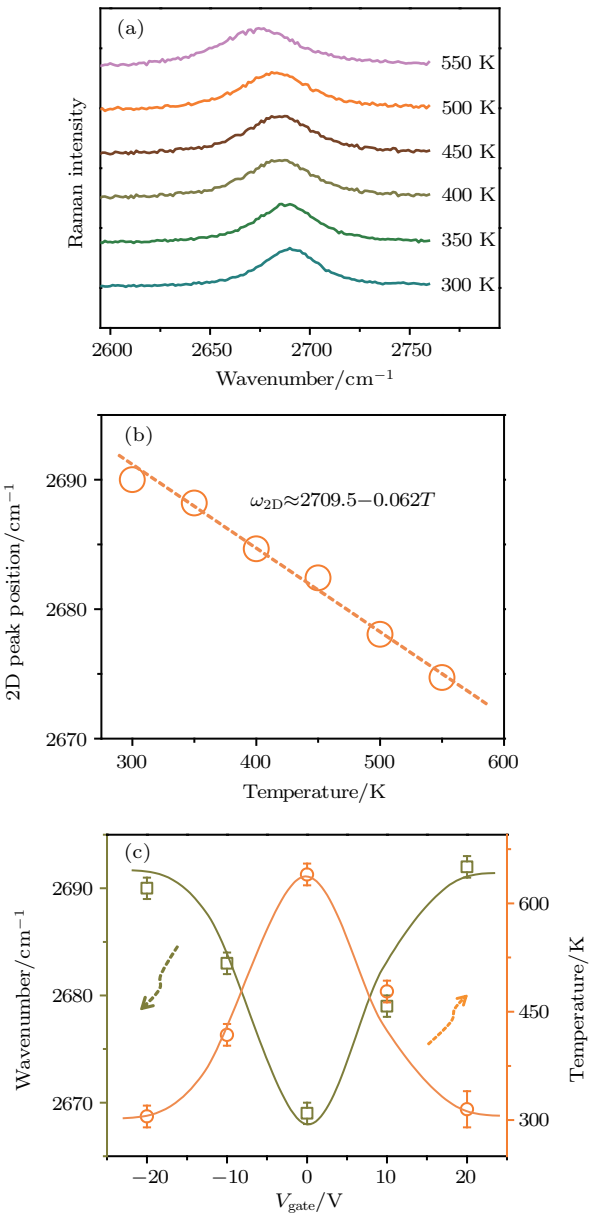


Fig. 4. (color online) (a) 2D peak region of the Raman spectra of the graphene heater shown in Fig. 3(b) at different temperatures. The excited laser is 633 nm. (b) Shift in 2D peak position extracted from panel (a). A linear formula $\omega_{2D} \approx 2709.5 - 0.062T$ is used to describe the relationship of the 2D peak position and temperature. The dashed line is a guide to the eyes. (c) The relationship of the 2D peak position and gate voltage when the heater is sourced with a current with a density of 4.5×10^7 A/cm^2. The temperatures of the graphene heater estimated from the above formula are also plotted. The solid lines are a guide to the eyes.

4. Conclusion

We report heating effects of CVD graphene devices operated at relatively high current density. Both Raman spectrum and test in breakdown current density indicate that CVD graphene has a very high current-carrying capacity similar to exfoliated graphene. We show that Joule heating geometrically increases with the increase of the current density while the modulability of the gate bias on Joule heating power decreases. It is found that the efficiency of heating is high in graphene nano-structures with a narrow and long channel. By measuring the Raman spectra, we find that the temperature of graphene varies with the back-gate voltage when a fixed current is sourced.

References

[1] Novoselov K S, Geim A K, Morozov S V, Jiang D, Zhang Y, Dubonos S V, Grigorieva I V and Firsov A A 2004 *Science* **306** 666
[2] Novoselov K S, Geim A K, Morozov S V, Jiang D, Katsnelson M I, Grigorieva I V, Dubonos S V and Firsov A A 2005 *Nature* **438** 197
[3] Zhang Y B, Tan Y W, Stormer H L and Kim P 2005 *Nature* **438** 201
[4] Li X L, Wang X R, Zhang L, Lee S W and Dai H J 2008 *Science* **319** 1229
[5] Han M Y, Özyilmaz B, Zhang Y B and Kim P 2007 *Phys. Rev. Lett.* **98** 206805
[6] Chen Z H, Lin Y M, Rooks M J and Avouris P 2007 *Physica E* **40** 228
[7] Moser J, Barreiro A and Bachtold A 2007 *Appl. Phys. Lett.* **91** 163513
[8] Murali R, Yang Y X, Brenner K, Beck T and Meindl J D 2009 *Appl. Phys. Lett.* **94** 243114
[9] Kang J, Kim H, Kim K S, Lee S, Bae S, Ahn J, Kim Y, Choi J and Hong B H 2011 *Nano Lett.* **11** 5154
[10] Sui D, Huang Y, Huang L, Liang J J, Ma Y F and Chen Y S 2011 *Small* **7** 3186
[11] Wang X F, Zhao H M, Yang Y and Ren T L 2017 *Chin. Phys. B* **26** 038501
[12] Lin S Y, Zhang T Y, Lu Q, Wang D Y, Yang Y, Wu X M and Ren T L 2017 *Rsc Advances* **43** 27001
[13] Zhang T Y, Zhao H M, Wang D Y, Wang Q, Pang Y, Deng N Q, Cao H W, Yang Y and Ren T L 2017 *Nanoscale* **9** 14357
[14] Sun J Y, Chen Y B, Priydarshi M K, Chen Z, Bachmatiuk A, Zou Z Y, Chen Z L, Song X J, Gao Y F, Rümmeli M H, Zhang Y F and Liu Z F 2015 *Nano Lett.* **15** 5846
[15] Freitag M, Steiner M, Martin Y, Perebeinos V, Chen Z H, Tsang J C and Avouris P 2009 *Nano Lett.* **9** 1883
[16] Chae D H, Krauss B, Klitzing K V and Smet J H 2009 *Nano Lett.* **10** 466
[17] Yeo J, Kim G, Hong S, Lee J, Kwon J, Lee H, Park H, Manoroktul W, Lee M and Lee B J 2014 *Small* **10** 5014
[18] Wu T R, Ding G Q, Shen H L, Wang H M, Sun L, Jiang D, Xie X M and Jiang M H 2013 *Adv. Funct. Mater.* **23** 198
[19] Incze P N, Osvath Z, Kamaras K and Biro L P 2008 *Carbon* **46** 1435
[20] Meric I, Han M Y, Young A F, Özyilmaz B, Kim P and Shepard K L 2008 *Nat. Nanotechnol.* **3** 654
[21] Barreiro A, Lazzeri M, Moser J, Mauri F and Bachtold A 2009 *Phys. Rev. Lett.* **103** 076601
[22] Blake P, Yang R, Morozov S V, Schedin F, Ponomarenko L A, Zhukov A A, Nair R R, Grigorieva I V, Novoselov K S and Geim A K 2009 *Solid State Commun.* **149** 1068
[23] Huard B, Stander N, Sulpizio J A and Gordon D G 2008 *Phys. Rev. B* **78** 121402
[24] Wang H M, Wu Y H, Cong C X, Shang J Z and Yu T 2010 *ACS Nano* **4** 7221
[25] Archanjo B S, Barboza A P M, Neves B R A, Malard L M, Ferreira E H M, Brant J C, Alves E S, Plentz F, Carozo V and Fragneaud B 2012 *Nanotechnology* **23** 255305
[26] Ferrari A C, Meyer J C, Scardaci V, Casiraghi C, Lazzeri M, Mauri F, Piscanec S, Jiang D, Novoselov K S and Roth S 2006 *Phys. Rev. Lett.* **97** 187401
[27] Ni Z H, Wang H M, Kasim J, Fan H M, Yu T, Wu Y H, Feng Y P and Shen Z X 2007 *Nano Lett.* **7** 2758
[28] Calizo I, Miao F, Bao W, Lau C N and Balandin A A 2007 *Appl. Phys. Lett.* **91** 071913
[29] Calizo I, Balandin A A, Bao W, Miao F and Lau C N 2007 *Nano Lett.* **7** 2645
[30] Ni Z H, Fan H M, Fan X F, Wang H M, Zheng Z, Feng Y P, Wu Y H and Shen Z X 2007 *J. Raman Spectrosc.* **38** 1449
[31] Huang F M, Yue K T, Tan P H, Zhang S L, Shi Z J, Zhou X H and Gu Z N 1998 *J. Appl. Phys.* **84** 4022
[32] Tian S B, Yang Y, Liu Z, Wang C, Pan R H, Gu C Z and Li J J 2016 *Carbon* **104** 27
[33] Zhou H Q, Qiu C Y, Yu F, Yang H C, Chen M J, Hu L J, Guo Y J and Sun L F 2011 *J. Phys. D: Appl. Phys.* **44** 185404
[34] Nef C, Pósa L, Makk P, Fu W Y, Halbritter A, Schönenberger C and Calame Michel 2014 *Nanoscale* **6** 7249
[35] Yan J, Zhang Y B, Kim P and Pinczuk A 2007 *Phys. Rev. Lett.* **98** 166802